Characterization of a Dual Josephson Impedance Bridge

Frédéric Overney[1], Nathan E. Flowers-Jacobs[2], Blaise Jeanneret[1], Alain Rüfenacht[2],
Anna E. Fox[2], Paul D. Dresselhaus[2] and Samuel P. Benz[2]
[1]Federal Institute of Metrology METAS, Lindenweg 50, 3003 Bern-Wabern, Switzerland
[2]National Institute of Standards and Technology, Boulder, CO 80305, USA

***Abstract*—This paper describes a dual Josephson impedance bridge capable of comparing any two impedances, that is, with any amplitude ratio and relative phase, over a wide range of frequency. A new, more compact, design has been achieved by mounting the two Josephson Arbitrary Waveform Synthesizers (dual JAWS) side-by-side in a single cryoprobe. We measured the crosstalk between the two JAWS sources and show that, by interchanging the impedances within the bridge, the effect of the crosstalk between JAWS sources can be reduced to a negligible level.**

***Index Terms*—Impedance comparison, AC Josephson voltage standard, Josephson Arbitrary Waveform Synthesizer, AC coaxial bridge.**

I. INTRODUCTION

The comparison of impedance standards using transformer-based bridges is widely used in national metrology institutes (NMIs) and allows the calibration of impedances with the highest accuracy in the audio frequency range [1], [2]. The major drawback of such bridges is that impedances can be compared only at a set of specific predefined magnitude ratios (typically 1:1 or 1:10) and relative phases (typically 0° or ±90°).

This limitation has been overcome by replacing the transformer with two ac Josephson voltage standards (also known as dual Josephson Arbitrary Waveform Synthesizers or dual JAWS sources), which generate accurate and stable voltages with a completely programmable magnitude ratio and relative phase. The first realization of an impedance bridge based on two JAWS circuits demonstrated the capability to compare any two kinds of impedances over the whole audio frequency range [3], [4].

Since the first realization of this Dual Josephson Impedance Bridge (DJIB) in 2016 [3], the system has been further optimized: the electronics [5] have been modified to make the system more compact [6] and the JAWS design has been improved to fit both sources in the same cryoprobe, which is cooled in a single helium Dewar. The preliminary description of this new dual source and the characterization of the new DJIB are presented in this summary.

II. DUAL JAWS SETUP

Fig. 1 represents schematically the wiring of the two JAWS sources located side-by-side in the cryoprobe. For clarity, the microwave circuitry is omitted. Each JAWS is composed of four arrays of 12 810 Josephson junctions (JJs) with critical currents of 10 mA. The JJs in each JAWS are driven by a single pulse generator channel; a four-way split is accomplished on-chip using two layers of Wilkinson dividers [6].

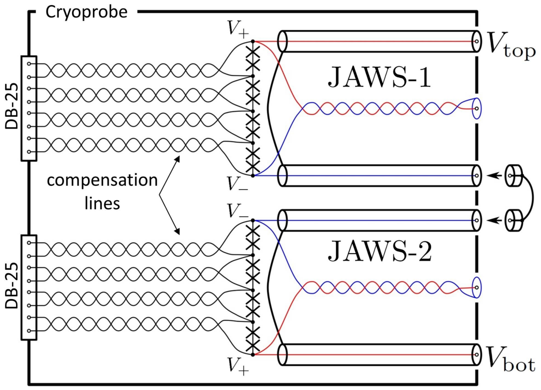

Fig. 1. Schematic representation of the low-frequency wiring of the two JAWS sources inside the cryoprobe. The grounding scheme of the circuit can be changed by connecting the grounding plugs shown near the V_- outputs on the right side of the figure.

For each JAWS, the inner conductor of each of two coaxial cables brings the audio-frequency quantum-accurate Josephson voltage (V_+ and V_-) from the chip to the top of the cryoprobe. The outer conductors of these coaxial cables are isolated from the cryoprobe and connected together near the chip. Each JAWS also has a pair of twisted wires connected in parallel with the coaxial cables for system testing (colored wires in Fig. 1). Four supplementary twisted-pair wires are connected from DB-25 connectors at the top of the cryoprobe to the four JJ arrays of each JAWS to provide the compensation current needed to generate voltages > 200 mV.

When the dual JAWS sources are implemented in the DJIB, the V_- outputs of the two JAWS circuits are connected together and shorted to ground using the grounding plugs shawn in Fig. 1. The V_+ outputs supply the quantum-accurate voltages V_{top} and V_{bot} to the bridge.

III. CROSSTALK

As described above, the two JAWS sources are located side by side. Although this configuration allows a more compact design, the question of crosstalk between the two JAWS circuits must be investigated in detail.

A. *Effect of crosstalk on the DJIB*

Fig. 2 shows schematically the effect of JAWS crosstalk on the DJIB. Once the bridge is balanced, i.e., no current is

U.S. Government work not protected by U.S. copyright

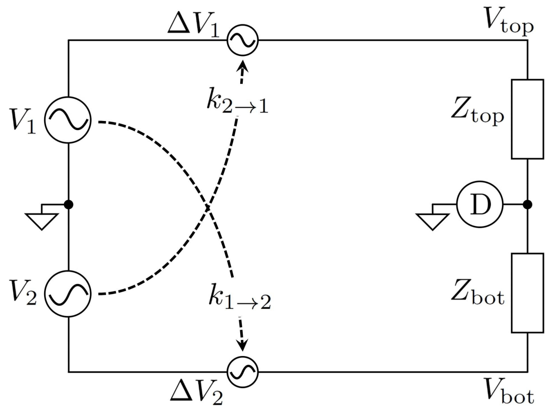

Fig. 2. Schematic representation of the cross-talk in the DJIB.

flowing through the detector D, the impedance ratio $Z_{\mathrm{bot}}/Z_{\mathrm{top}}$ is determined by the voltage ratio $V_{\mathrm{bot}}/V_{\mathrm{top}}$. The crosstalk will induce a deviation in V_{bot} from the JAWS signal V_2 by a quantity $\Delta V_2 = k_{1\to 2}V_1$ where $k_{1\to 2}$ is the crosstalk coefficient. Similarly, V_{top} will differ from V_1 by $\Delta V_1 = k_{2\to 1}V_2$.

We first consider the case of symmetric crosstalk $k_{1\to 2} = k_{2\to 1} = k$, where k is complex and $|k| << 1$. The balance equation is then given by:

$$\frac{Z_{\mathrm{bot}}}{Z_{\mathrm{top}}} = -\frac{V_{\mathrm{bot}}}{V_{\mathrm{top}}} = -r\frac{1+k\frac{1}{r}}{1+kr} \approx -r\Big(1+k(\frac{1}{r}-r)\Big), \quad (1)$$

where $r = V_2/V_1$ is the ratio of quantum-accurate reference voltages. Eq. 1 clearly shows that the crosstalk has a negligible effect when comparing impedances of the same kind (R to R or C to C) in a 1:1 ratio (i.e.: $r \approx 1$). However, when the ratio differs from 1, the effect of the crosstalk must be taken into account.

It has been shown [3] that one of the unique and important properties of the DJIB is the ability to repeat the balance of the bridge with the two impedance standards inverted, even with $r \neq 1$. The inverted balance of the bridge leads to the following equation:

$$\frac{Z_{\mathrm{top}}}{Z_{\mathrm{bot}}} = -\tilde{r}\frac{1+k\frac{1}{\tilde{r}}}{1+k\tilde{r}}, \quad (2)$$

where $\tilde{r}$ is the new generated voltage ratio $\tilde{V_2}/\tilde{V_1}$. Combining Eq. 1 and Eq. 2, the impedance ratio is finally given by

$$\frac{Z_{\mathrm{top}}}{Z_{\mathrm{bot}}} \approx \sqrt{\frac{r}{\tilde{r}}\Big(1+k^2(\frac{1}{r^2}-r^2)\Big)}, \quad (3)$$

assuming that $\tilde{r} \approx 1/r$. Eq. 3 clearly shows the advantage of performing both the direct and reverse measurements: the impact of the crosstalk is reduced to second order.

B. Measurement of the crosstalk coefficients

To determine the crosstalk coefficient k, the voltage ΔV_2 was measured at frequencies between 1 kHz to 50 kHz, with the amplitude of V_2 set to zero and the rms amplitude of V_1 set to 1 V. The amplitude $|\Delta V_2|$ increases linearly with frequency and reaches an rms amplitude between 1.4 μV and 130 μV at 50 kHz, depending on the DJIB grounding scheme. The smallest crosstalk coefficient of 1.4 μV was obtained when both JAWS sources were completely floating, i.e., when the two short-circuit plugs of Fig. 1 were not connected together.

The origin of the crosstalk appears to be the capacitive current that flows from one JAWS source to the other, either between on-chip elements or between various twisted-pair wires connecting the JAWS chip to the top of the cryoprobe. This capacitive current, $j\omega CV_1$, needs to return to ground through the impedance of the link between JAWS-2 and JAWS-1, $z = R_s + j\omega L_s$. It produces a voltage drop $\Delta V_2 = j\omega CV_1 z$. The impedance z includes the on-chip impedance of the JJ arrays and superconducting wiring plus the series impedance of the coaxial cables. Because the same capacitance C and impedance z are involved in the reverse coupling, the hypothesis of a symmetric crosstalk coefficient is fully justified. We used a four-wire measurement to determine the total output impedance, $R_s = 2.5\ \Omega$ and $L_s = 2.6\ \mu$H, which implies that a coupling capacitance between the JAWS sources of $C = 160$ pF would be required to explain the maximum measured crosstalk of $\Delta V_2 = 130\ \mu$V at 50 kHz.

This explanation for the crosstalk is further supported by the fact that the phase of the measured voltage ΔV_2 is shifted by roughly 90° relative to the phase of V_1. Moreover, when the two JAWS circuits are completely floating, the capacitive current vanishes because there is no path back to the source.

IV. CONCLUSION

Mounting the two JAWS sources side-by-side in a single cryoprobe results in a simple, compact, dual Josephson source. However, this configuration requires careful measurement of crosstalk and accounting for the effect of the crosstalk on the calculated voltage ratio, especially when the ratio differs from 1. By combining both direct and reverse measurements, the effect of the crosstalk on the calculated voltage ratio is reduced to second order and does not significantly contribute to the ratio, even though the coupling between the two JAWS circuits is as large as 160 pF. The next step for the DJIB is to detremine a full uncertainty budget and directly compare it to a high-accuracy transformer-based bridge.

REFERENCES

[1] B. Hague and T. R. Foord, *Alternating Current Bridge Methods*. Pitman Publishing, 1971.

[2] S. A. Awan, B. Kibble, and J. Schurr, *Coaxial Electrical Circuits for Interference-Free Measurements*, ser. IET Electrical Measurement Series. Institution of Engineering and Technology, Jan 2011.

[3] F. Overney *et al.*, “Josephson-based full digital bridge for high-accuracy impedance comparisons,” *Metrologia*, vol. 53, no. 4, pp. 1045–1053, Aug 2016.

[4] S. Bauer *et al.*, “A novel two-terminal-pair pulse-driven Josephson impedance bridge linking a 10 nF capacitance standard to the quantized Hall resistance,” *Metrologia*, vol. 54, no. 2, pp. 152–160, Apr 2017.

[5] S. P. Benz and S. B. Waltman, “Pulse-Bias Electronics and Techniques for a Josephson Arbitrary Waveform Synthesizer,” *IEEE Transactions on Applied Superconductivity*, vol. 24, no. 6, pp. 1–7, Dec 2014.

[6] N. E. Flowers-Jacobs, S. B. Waltman, A. E. Fox, P. D. Dresselhaus, and S. P. Benz, “Josephson Arbitrary Waveform Synthesizer With Two Layers of Wilkinson Dividers and an FIR Filter,” *IEEE Transactions on Applied Superconductivity*, vol. 26, no. 6, pp. 1–1, sep 2016.